Connection of translational and rotational dynamical heterogeneities with the breakdown of the Stokes-Einstein and Stokes-Einstein-Debye relations in water

Marco G. Mazza,[1] Nicolas Giovambattista,[2] H. Eugene Stanley,[1] and Francis W. Starr[3]

[1]*Center for Polymer Studies and Department of Physics, Boston University, Boston, Massachusetts 02215, USA*
[2]*Department of Chemical Engineering, Princeton University, Princeton, New Jersey 08544-5263, USA*
[3]*Department of Physics, Wesleyan University, Middletown, Connecticut 06459, USA*

We study the Stokes-Einstein (SE) and the Stokes-Einstein-Debye (SED) relations, $D_t = k_B T / 6\pi\eta R$ and $D_r = k_B T / 8\pi\eta R^3$, where D_t and D_r are the translational and rotational diffusivity, respectively, T is the temperature, η the viscosity, k_B the Boltzmann constant, and R the "molecular" radius. Our results are based on molecular dynamics simulations of the extended simple point charge model of water. We find that both the SE and SED relations break down at low temperature. To explore the relationship between these breakdowns and dynamical heterogeneities (DHs), we also calculate the SE and SED relations for subsets of the 7% "fastest" and 7% "slowest" molecules. We find that the SE and SED relations break down in both subsets, and that the breakdowns occur on all scales of mobility. Thus these breakdowns appear to be generalized phenomena, in contrast with a view where only the most mobile molecules are the origin of the breakdown of the SE and SED relations, embedded in an inactive background where these relations hold. At low temperature, the SE and SED relations in both subsets of molecules are replaced with "fractional" SE and SED relations, $D_t \sim (\tau/T)^{-\xi_t}$ and $D_r \sim (\tau/T)^{-\xi_r}$, where $\xi_t \approx 0.84 (<1)$ and $\xi_r \approx 0.75 (<1)$. We also find that there is a decoupling between rotational and translational motion, and that this decoupling occurs in both the fastest and slowest subsets of molecules. Further, we find that, the decoupling increases upon cooling, but that the probability of a molecule being classified as both translationally and rotationally fastest also increases. To study the effect of time scale for SE and SED breakdown and decoupling, we introduce a time-dependent version of the SE and SED relations, and a time-dependent function that measures the extent of decoupling. Our results suggest that both the decoupling and SE and SED breakdowns originate at a time scale corresponding to the end of the cage regime, when diffusion starts. This is also the time scale when the DHs are more relevant. Our work also demonstrates that selecting DHs on the basis of translational or rotational motion more strongly biases the calculation of diffusion constants than other dynamical properties such as relaxation times.

I. INTRODUCTION

At temperatures where liquids have a diffusion constant similar to that of ambient temperature water, the translational and rotational diffusion, D_t and D_r respectively, are well described by the Stokes-Einstein (SE) relation [1]

$$D_t = \frac{k_B T}{6\pi\eta R} \qquad (1)$$

and the Stokes-Einstein-Debye (SED) relation [2]

$$D_r = \frac{k_B T}{8\pi\eta R^3}. \qquad (2)$$

Here T is the temperature, η the viscosity, k_B the Boltzmann constant, and R the "molecular" radius. These equations are derived by a combination of classical hydrodynamics (Stokes law) and simple kinetic theory (e.g., the Einstein relation) [3]. Recently, the limits of the SE and SED relations have been an active field of experimental [4–9], theoretical [10–17], and computational [18–30] research. The general consensus is that the SE and SED relations hold for low-molecular-weight liquids for $T \gtrsim 1.5 T_g$, where T_g is the glass transition temperature. For $T \lesssim 1.5 T_g$, deviations from either one or both of the SE and SED relations are observed. Experimentally, it is found that the SE relation holds for many

liquids in their stable and weakly supercooled regimes, but when the liquid is deeply supercooled it overestimates D_t relative to η by as much as two or three orders of magnitude, a phenomenon usually referred to as the "breakdown" of the SE relation. The situation for the SED relation is more complex. Some experimental studies found agreement with the predicted values of the SED relation even for deeply supercooled liquids [7,31,32], while others claim also a breakdown of the SED relation to the same extent as for the SE relation [5,33–36]. The failure of these relations provides a clear indication of a fundamental change in the dynamics and relaxation of the system. Indeed, the changing dynamics of the liquid as it approaches the glass transition is well documented, but not yet fully understood [37–40].

There is a growing body of evidence [41–46] that, upon cooling, a liquid does not become a glass in a spatially homogeneous fashion. Instead the system is characterized by the appearance of dynamical heterogeneities [31,32,41–56]. This phenomenon is often called "spatially heterogeneous dynamics," since there are spatial regions in which the structural relaxation time can differ by orders of magnitude from the average over the entire system [57]. In the dynamical heterogeneities (DHs) view, the motion of atoms or molecules is highly spatially correlated. The presence of these DHs has been argued to give rise to the breakdown of the SE relation [10,15]. Since the derivation of the Einstein relation

assumes uncorrelated motion of particles, it is reasonable that the emergence of correlations could result in a failure of the SE relation. The aim of the present work is to assess the validity of the SE and SED relations in the extended simple point charge (SPC/E) model of water, and consider to what extent the DHs contribute to the SE and SED breakdown.

Computer simulations have been particularly useful for studying DHs (e.g., see Refs. [58–65]) since simulations have direct access to the details of the molecular motion. For water, the existence of regions of enhanced or reduced mobility has also been identified [63,66]. In particular, Ref. [63] identifies the clusters of molecules with greater *translational* (or center of mass) mobility with the hypothesized "cooperatively rearranging regions" of the Adam-Gibbs approach [67,68]. For water, those DHs are also accompanied by spatial heterogeneities [69,70].

Most computer simulation studies on DHs describe these heterogeneities based on the particle or molecule translational degrees of freedom. We will refer to these DHs as translational heterogeneities (THs). For water, it is also necessary to consider the rotational degrees of freedom of the molecule. Recently, some computer simulation studies on molecular systems described the DHs based on the molecular *rotational* degrees of freedom [4,18,20,71–74]. We will refer to these DHs as rotational heterogeneities (RHs). For the case of a molecular model of water, RHs were studied [74] and it was found that RHs and THs are spatially correlated. This work extends those results. We find support for the idea that THs are connected to the failure of the SE relation, and further that RHs have a similar effect on SED relation. Additionally, we find that the breakdown of these relations is accompanied by the decoupling of the translational and rotational motion.

This work is organized as follows. In the next section we describe the water model and simulation details. In Secs. III and IV we test the validity of the SE and SED relations and their connection with the presence of DH, respectively. The decoupling between rotational and translation motion is studied in Sec. V. In Sec. VI we explore the role of time scale in the breakdown of the SE and SED relations and decoupling of rotational and translational motion. We summarize our results in Sec. VII. We have placed some technical aspects of the work in Appendices to facilitate the flow of our results.

II. MODEL AND SIMULATION METHOD

We perform molecular dynamics (MD) simulations of the SPC/E model of water [75]. This model assumes a rigid geometry for the water molecule, with three interaction sites corresponding to the centers of the hydrogen (H) and oxygen (O) atoms. Each hydrogen has a charge $q_H = 0.4238e$, and the oxygen charge is $q_O = -2.0q_H$, where e is the magnitude of the electron charge. The OH distance is 1.0 Å and the HOH angle is 109.47°, corresponding to the tetrahedral angle. In addition to the Coulombic interactions, a Lennard-Jones interaction is present between oxygen atoms of two different molecules; the Lennard-Jones parameters are $\sigma = 3.166$ Å and $\epsilon = 0.6502$ kJ/mol. We use a cutoff distance of $2.5\sigma = 7.915$ Å for the pair interactions, and the reaction field

technique [76] is used to treat the long-range Coulombic interactions.

We perform simulations with constant particle number N, volume V, and temperature T with $N = 1728$ water molecules and fixed density $\rho = 1.0$ g/cm^3. The values of the simulated temperature are $T = 210$, 220, 230, 240, 250, 260, 270, 280, 290, 300, 310, 330, and 350 K. We use the Berendsen method [77] to keep the temperature constant [78]. We use periodic boundary conditions and a simulation time step of 1 fs. To ensure that simulations attain a steady-state equilibrium, we perform equilibration simulations for at least the duration specified by Ref. [79]. After these equilibration runs we continue with production runs of equal duration during which we store the coordinates of all atoms for data analysis. To improve the statistics of our results, we have performed five independent simulations for each T. Reference [79] provides further details of the simulation protocol.

III. BREAKDOWN OF THE STOKES-EINSTEIN AND STOKES-EINSTEIN-DEBYE RELATIONS

To assess the validity of the SE and SED relations we consider a simple rearrangement of Eqs. (1) and (2), i.e., we define the SE ratio

$$R_{SE} \equiv \frac{D_t \eta}{T} \qquad (3)$$

and the SED ratio

$$R_{SED} \equiv \frac{D_r \eta}{T}. \qquad (4)$$

Both R_{SE} and R_{SED} will be temperature independent if the SE and SED relations are valid.

To evaluate R_{SE} and R_{SED}, we must first calculate the appropriate diffusion constants. Following normal procedure, we define

$$D_t \equiv \lim_{\Delta t \to \infty} \frac{1}{6\Delta t} \langle r^2(\Delta t) \rangle, \qquad (5)$$

where $\langle r^2(\Delta t) \rangle$ is the translational mean square displacement (MSD) of the oxygen atoms

$$\langle r^2(\Delta t) \rangle \equiv \frac{1}{N} \sum_{i=0}^{N} |\vec{r}_i(t') - \vec{r}_i(t)|^2. \qquad (6)$$

Here, $\vec{r}_i(t)$ and $\vec{r}_i(t')$ are the positions of the oxygen atom of molecule i at times t and t', respectively, and $\Delta t = t' - t$. Analogously, we define the rotational diffusion coefficient

$$D_r \equiv \lim_{\Delta t \to \infty} \frac{1}{4\Delta t} \langle \varphi^2(\Delta t) \rangle, \qquad (7)$$

where $\langle \varphi^2(\Delta t) \rangle$ is the rotational mean square displacement (RMSD) for the vector rotational displacement $\vec{\varphi}_i(\Delta t)$. Special care must be taken to calculate $\langle \varphi^2(\Delta t) \rangle$ so that it is unbounded. A detailed discussion of this procedure is provided in Appendix A.

We also need the viscosity η to evaluate R_{SE} and R_{SED}. Unfortunately, accurate calculation of η is computationally
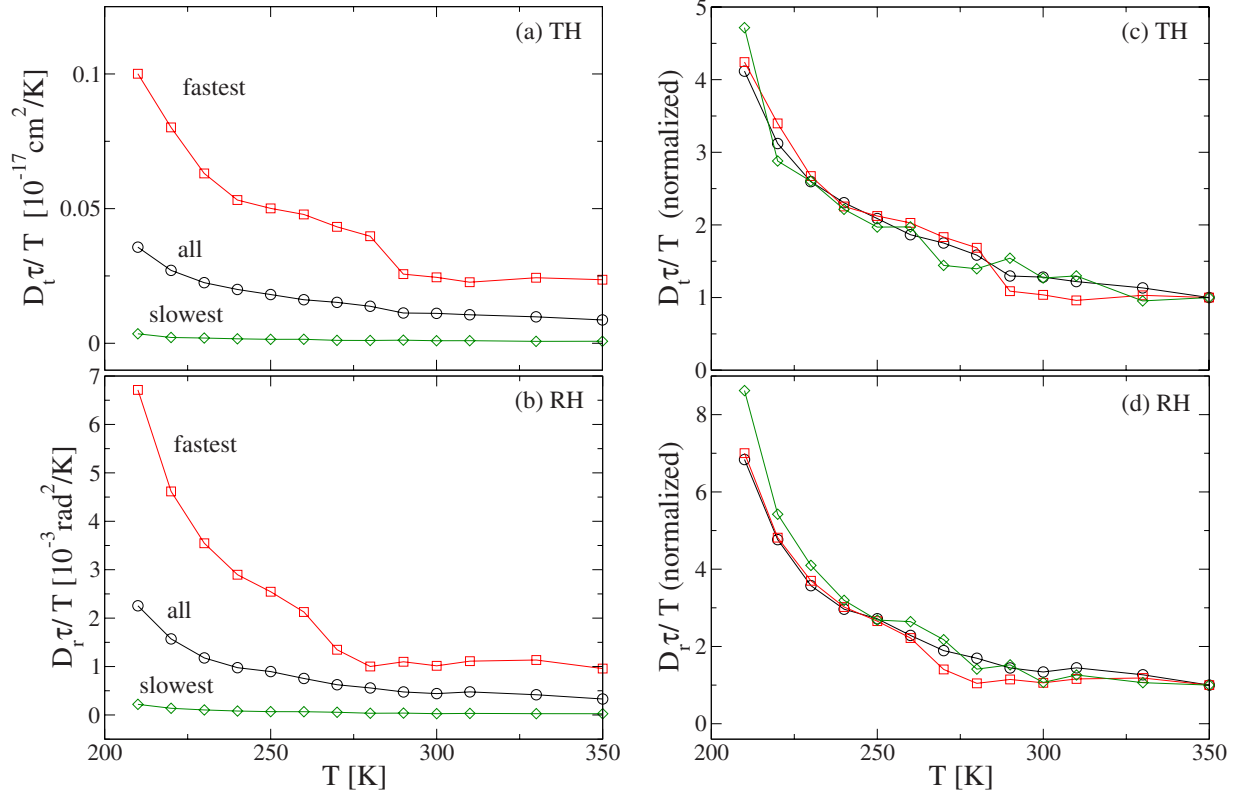
FIG. 1. (Color online) (a) Stokes-Einstein ratio $D_t\tau/T$ for the 7% most translationally mobile molecules (fastest), for the 7% least translationally mobile molecules (slowest), and for the entire system (all). There is a breakdown of the Stokes-Einstein relation (constant Stokes-Einstein ratio) at low temperatures in both the fastest and slowest subsets, as well as for the entire system. (b) Stokes-Einstein-Debye ratio $D_r\tau/T$ for the 7% most rotationally mobile molecules, for the 7% least rotationally mobile molecules, and for the entire system (all). As in (a), there is a breakdown of the Stokes-Einstein-Debye relation (constant Stokes-Einstein-Debye ratio). (c) and (d) Normalization of the curves in (a) and (b), respectively, by the corresponding quantities at $T=350$ K. The collapse of these curves demonstrates that the relative deviations from the Stokes-Einstein and Stokes-Einstein-Debye relations are approximately the same for the corresponding mobility subsets.

challenging. A frequently employed approximation exploits the fact that η is proportional to the shear stress relaxation time τ_s, via the infinite frequency shear modulus G_∞, which is nearly T independent [80]. Additionally, we expect that τ_s (a "collective property") should be nearly proportional to other collective relaxation times, such as the relaxation time τ defined from the coherent intermediate scattering function, $F(q,\Delta t)$, where q is the wave vector. Therefore, we substitute η by τ, which should affect only the value and units of the constants in R_{SE} and R_{SED}. For the purposes of our calculations, we define τ by fitting $F(q,\Delta t)$ at long times with a "stretched" exponential

$$F(q,\Delta t) \sim \exp[-(\Delta t/\tau)^\beta], \qquad (8)$$

where $0<\beta<1$, and we focus on the q value corresponding to the first peak in the static structure factor $S(q)$.

Now that we have the necessary quantities, we show R_{SE} and R_{SED} in Figs. 1(a) and 1(b) with the curves labeled "all." Both quantities deviate at low T from the corresponding constant values reached at high temperature, indicating a breakdown of both the SE and SED relations.

Whether there is a breakdown of the SED relation in experiments is not clear. While some experiments measuring

dipole relaxation times show that the SED relation holds down to the glass transition [31,32], other experiments [81] show that the SED relation fails for low T. Our simulations are in agreement with the breakdown of the SED ratio observed in, e.g., Ref. [22,82]. Figures 1(a) and 1(b) also show R_{SE} and R_{SED} for different subsets of molecules to examine the role played by DH. This is discussed in the following section.

IV. ROLE OF DYNAMICAL HETEROGENEITIES

A. Identifying mobility subsets

Some theoretical approaches (e.g., [10,15]) attempt to explain the breakdown of SE and/or SED in terms of DH. To this end, we must first describe the procedure used to select molecules whose motion (or lack thereof) is spatially correlated. A variety of approaches have been used to probe the phenomenon of DH. Here we use one of the most common techniques: partitioning a system into mobility groups based on their rotational or translational maximum displacement.

For the TH, we define the translational mobility μ_i of a molecule i at a given time t_0 and for an observation time Δt, as the maximum displacement over the time interval $[t_0, t_0 + \Delta t]$ of its oxygen atom [83]

$$\mu_i(t_0, \Delta t) \equiv \max\{|\vec{r}_i(t+t_0) - \vec{r}_i(t_0)|, \ t_0 \leq t \leq t_0 + \Delta t\}. \quad (9)$$

For the RH, following [74], we define a rotational mobility that is analogous to the translational case. In analogy with Eq. (9), we define the rotational mobility at time t_0 with an observation time Δt as

$$\psi_i(t_0, \Delta t) \equiv \max\{|\vec{\varphi}_i(t+t_0) - \vec{\varphi}_i(t_0)|, \ t_0 \leq t \leq t_0 + \Delta t\}. \quad (10)$$

We identify the subsets of rotationally and translationally "fastest" molecules as the 7% of the molecules with largest ψ_i and μ_i, respectively. Analogously, we identify the subsets of rotationally and translationally "slowest" molecules as the 7% of the molecules with smallest ψ_i and μ_i, respectively. The choice of 7% is made to have a direct comparison with the analysis of Refs. [63,74], but the qualitative details of our work are unaffected by modest changes in this percentage. In the following, we will refer to these subsets of molecules as TH and RH, fastest and slowest, depending on whether we consider the top or the bottom of the distribution of mobilities. We will see that comparing the fastest and the slowest molecules will reveal new features of DH.

B. Stokes-Einstein and Stokes-Einstein-Debye relations for fastest and slowest molecules

Having identified subsets of highly mobile or immobile molecules, we can calculate the ratios R_{SE} and R_{SED} by limiting the evaluation of D_t, D_r, and τ to these subsets. This is relatively straightforward for the diffusion constants, since they depend only on single-molecule averages. For τ, the situation is more complex since $F(q, \Delta t)$ includes cross correlations between molecules. Hence we specialize the definition of $F(q, \Delta t)$ for the TH and RH subsets by introducing a definition that captures the cross correlation within subsets and between a subset and the rest of the system. We call this function $F_{subset}(q, \Delta t)$, which we discuss in detail in Appendix B.

We show the values of R_{SE} and R_{SED} in Figs. 1(a) and 1(b) for the cases when only the fastest and slowest subsets of molecules are considered. Like the total system average, both the SE and SED ratios for the subsets deviate at low T from the corresponding constant values reached at high temperature. Therefore, we observe that the breakdowns of both the SE and SED relations occur not only in the subset of the fastest molecules, but also in the slowest. We have also confirmed a breakdown in intermediate subsets.

The most mobile subset of molecules has a consistently greater value of $D_t \tau/T$ and $D_r \tau/T$ than the rest of the system, while the ratios for the least mobile subsets are always smaller. This is a result of the fact that the means by which we select the different subsets most strongly affects the diffusion constant (see Appendix B), and hence the differences in the SE and SED ratios between the full system and the subsets are dominated by the diffusion constant, rather than by the relaxation time.

In order to compare the relative deviations of these curves from the SE and SED predictions, we normalize R_{SE} and R_{SED} by their respective high-temperature values [Figs. 1(c)

and 1(d)]. We observe that there is a collapse of all the curves; thus, we conclude that both the most and least mobile molecules contribute in the same fashion to the breakdown of the SE and SED relationships. Moreover, this result supports the scenario that the deviation from the SE and SED relations cannot be attributed to only one particular subset of fastest or slowest molecules, but to all scales of translational and rotational mobility [22]. We have confirmed this by looking at subsets of intermediate mobility (not shown). Therefore, we interpret our results as a sign of a "generalized breakdown" in the system under study, in contrast to a picture where only the most mobile molecules are the origin of the breakdown of SE and SED relations, embedded in an inactive background where the SE and SED equations hold (see, e.g., [7]). These results are consistent with the results of Ref. [22], whose authors arrived at the same conclusion via a different analysis.

C. Fractional Stokes-Einstein and Stokes-Einstein-Debye relations

When the SE and SED relations fail, it is frequently observed that they can be replaced by *fractional* functional forms [4,6,33,84–89]

$$D_t \sim \left(\frac{\tau}{T}\right)^{-\xi_t}, \quad D_r \sim \left(\frac{\tau}{T}\right)^{-\xi_r} \quad (11)$$

with $\xi_t < 1$ and $\xi_r < 1$. Hence we test to what degree Eqs. (11) hold for our system. In Fig. 2 we show a parametric plot of diffusivity versus τ/T for the entire system, and for the fastest and slowest molecules composing the TH and RH. The results at low temperature are well fitted with the fractional form of SE and SED relations. From Fig. 2, ξ_t for TH is 0.83, 0.84, and 0.84 for fastest, slowest, and all, respectively, so all TH have approximately the same exponent. Similarly, for RH we find that ξ_r is 0.75, 0.76, and 0.75 for fastest, slowest, and all, respectively.

Reference [22] found a stronger form of this fractional relation. Specifically, Ref. [22] examined an "ensemble" of systems of the ST2 water model [90] at the same T, which by statistical variation have fluctuations in the SE and SED ratios. Nonetheless, all systems collapsed to the same master curve when plotted in the parametric form shown in Fig. 2, meaning that the systems dominated by mobile or immobile molecules collapse to the same curve. While Ref. [22] employed a very different method (small systems followed for shorter times), the conclusion of our Fig. 2 is the same: a generalized deviation from the SE and SED relations. However, Fig. 2 clearly shows that we do not find a general collapse in our present calculation. To understand why, we return to the fact that the method by which we define mobility affects much more strongly the diffusion constants than the coherent relaxation time τ. As a result, it is impossible to have the results for the mobile and immobile subsets to collapse to a single master curve. To observe the same collapse, presumably one needs a more "neutral" method for selecting the mobile particles—that is, one that does not explicitly bias toward a specific property. Unfortunately, such an approach is not obvious. However, we reproduced the ensemble ap-
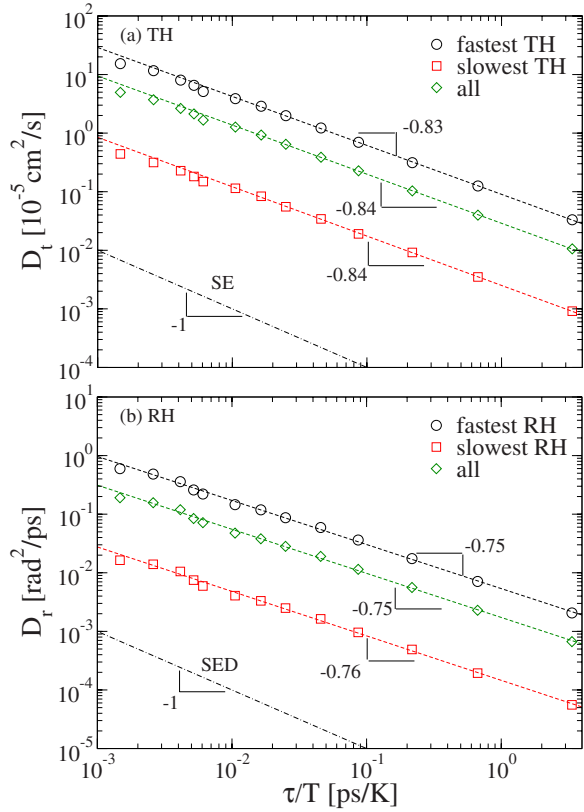
FIG. 2. (Color online) (a) Power-law fits of translational diffusivity D_t as functions of τ/T, $D_t \sim (\tau/T)^{-\xi_t}$, for the eight values of temperature $T = 210, \ldots, 280$ K (but not for the remaining values $T = 290, \ldots, 350$ K), for fastest translational heterogeneities (TH), slowest TH, and all molecules. We estimate $\xi_t \approx 0.84$. The dot-dashed line represents the normal Stokes-Einstein behavior ($\xi_t = 1$). Consistently with the results of Fig. 1, the deviation of these three curves from the Stokes-Einstein behavior is almost identical as reflected in the values of these fractional exponents. (b) Power-law fits of rotational diffusivity D_r as functions of τ/T, $D_r \sim (\tau/T)^{-\xi_r}$, of simulations in the same temperature range as in (a) for fastest rotational heterogeneities (RH), slowest RH, and all molecules. We estimate $\xi_r \approx 0.75$. The dot-dashed line represents the normal Stokes-Einstein-Debye behavior ($\xi_r = 1$). Also for RH, a fractional law is found with the same exponents for the three families considered, and, noticeably, the deviation from the normal case ($\xi_r = 1$) is stronger for D_r than for D_t, since $\xi_r < \xi_t$.

proach of Ref. [22], by splitting each of our five simulations into three trajectories. We obtain reasonable fluctuations that allow us to test and confirm (not shown) the observation of collapse of Ref. [22]. Hence, the phenomenon of homogeneous breakdown of the SE and SED relations appears to be robust for the different water models.

V. DECOUPLING OF TRANSLATIONAL AND ROTATIONAL MOTIONS

The SE and SED relations also imply a coupling between rotational and translational motion. Specifically, Eqs. (1) and (2) imply that the ratio
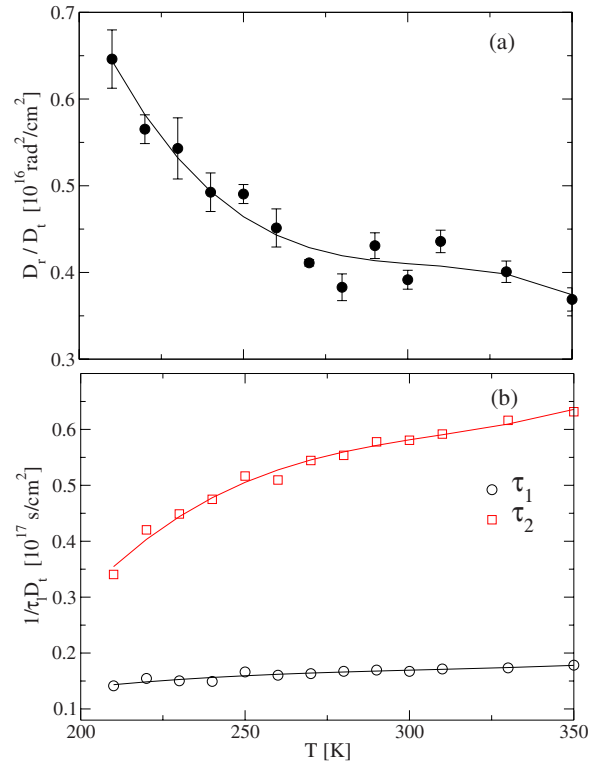

FIG. 3. (Color online) (a) Ratio of rotational and translational diffusivities D_r/D_t as a function of temperature. As temperature decreases, this ratio increases, indicating a decoupling between rotation and translational motion. The deviation of D_r is stronger than that of D_t. The line is a guide for the eye. (b) Same as (a) where the rotational diffusivity D_r is replaced by the inverse of the rotational relaxation time τ_ℓ with $\ell = 1, 2$, as is usually done in experiments. An opposite decoupling is observed in (a) and (b). The lines are guides for the eye.

$$\frac{D_r}{D_t} = \frac{3}{4R^2} \tag{12}$$

should remain constant as a function of temperature. Since we have already seen that the SE and SED ratios are not obeyed, it is likely that the ratio D_r/D_t is also violated [91]. However, it is also possible that D_r/D_t remains constant if both D_r and D_t deviate from their expected behavior in the same way.

Figure 3(a) shows D_r/D_t as a function of temperature. As T decreases, we observe that D_r/D_t increases, which implies that the breakdown of the SED relation is more pronounced than that of the SE relation.

Experiments generally do not examine the behavior of D_r/D_t since D_r is not accessible. Instead, D_r is usually replaced by $(\tau_\ell)^{-1}$ with $\ell = 2$ [19]. Here, τ_ℓ is the relaxation time of the rotational correlation function

$$C_\ell(\Delta t) \equiv \langle P_\ell \{ \cos[\hat{p}(t) \cdot \hat{p}(t + \Delta t)] \} \rangle, \tag{13}$$

where $P_\ell(x)$ is the Legendre polynomial of order ℓ, and $\hat{p}(t)$ is defined in Appendix A. Figure 3(b) shows $(\tau_\ell)^{-1}/D_t$ for $\ell = 1, 2$. We observe that $(\tau_\ell)^{-1}/D_t$ also shows a decoupling between rotational and translational motion. However, while
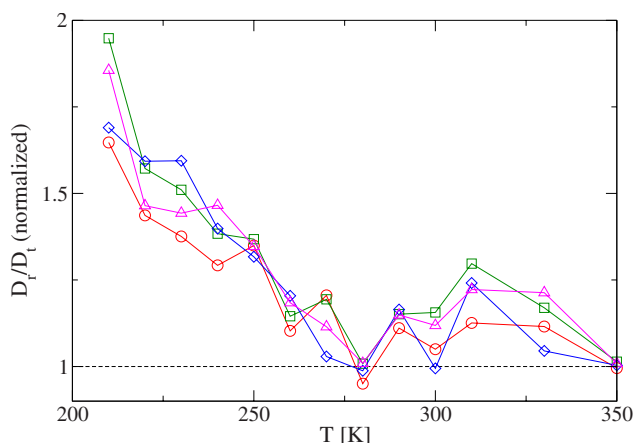
FIG. 4. (Color online) Ratio of rotational and translational diffusivities, D_r and D_t respectively, for the following choices of subsets: D_r for fastest translational heterogeneities (TH) divided by D_t for fastest TH ($\diamond$), D_r for slowest TH divided by D_t for slowest TH ($\triangle$), D_r for fastest rotational heterogeneities (RH) divided by D_t for fastest RH ($\bigcirc$), D_r for slowest RH divided by D_t for slowest RH ($\square$). The values were normalized by the $T=350$ K values for every curve. The fact that for these four cases D_r/D_t deviates from unity (dashed line) to approximately the same degree indicates that the decoupling occurs across all four cases.

D_r/D_t *increases* upon cooling, $(\tau_\ell)^{-1}/D_t$ *decreases* upon cooling. MD simulations using an *ortho*-terphenyl (OTP) model [92] and the ST2 water model [22] also find a qualitatively similar temperature dependence of decoupling of the SE and SED relations depending on whether D_r or τ_2 is used. In the simulations of OTP, it was shown that D_r/D_t starts to increase upon cooling at the same temperature at which caging in rotational motion becomes relevant; this caging results in intermittent large rotations that are not accounted for by the Debye approximation.

Similar to the analysis of the breakdown of the SE and SED ratios, we can test whether DHs play a strong role in the decoupling by examining the ratio D_r/D_t for the different mobility subsets. This is slightly complicated by the fact that we can choose mixed mobility subsets when calculating the ratio. Figure 4 shows that the ratios D_r/D_t for all choices of mobility subsets approximately coincide when scaled by the high-temperature behavior of D_r/D_t. This indicates that (like the breakdown of the SE and SED relations) the decoupling is uniform across the subsets of mobility.

VI. TIME SCALES FOR BREAKDOWN AND DECOUPLING

A. Time-dependent Stokes-Einstein and Stokes-Einstein-Debye relations

The SE and SED relations depend on D and η, which are defined only in the asymptotic limit of infinite time. In contrast, the time scale on which DH exist is finite, and generally shorter than the time scale on which the system becomes diffusive. As a result, making the connection between DH and the breakdown of SE and SED expressions is difficult. To address this complication, we incorporate a time dependence in the SE and SED relations, so that we can evaluate

these relations at the time scale of the DH. This point has been neglected so far in the literature. To define time-dependent versions of the SE and SED ratios, we first define time-dependent diffusivities

$$D_t(\Delta t) \equiv \frac{\langle r^2(\Delta t)\rangle}{6\Delta t}, \quad D_r(\Delta t) \equiv \frac{\langle \varphi^2(\Delta t)\rangle}{4\Delta t}, \tag{14}$$

and we also define time-dependent relaxation times

$$\tau(\Delta t) \equiv \int_t^{t+\Delta t} F(q,t')dt'. \tag{15}$$

Note that $D_t(\Delta t) \rightarrow D_t$ and $D_r(\Delta t) \rightarrow D_r$ in the limit $\Delta t \rightarrow \infty$. The definition of $\tau(\Delta t)$ requires some explanation: $\tau(\Delta t)$ is the time integral of the intermediate scattering function, and $\tau(\Delta t)$ will be proportional to the standard relaxation time τ [Eq. (8)] in the limit $\Delta t \rightarrow \infty$. There is a constant of proportionality resulting from the stretched exponential form [93]. When, instead, DH are considered, $F_{subset}(q,\Delta t)$ [see Eq. (B2)] is used in the computation of $\tau(\Delta t)$. We choose these definitions since, in the limit $\Delta t \rightarrow \infty$, they converge or are proportional to the corresponding time-independent definitions. We will use these time-dependent quantities to examine time-dependent generalizations of R_{SE} [Eq. (3)] and R_{SED} [Eq. (4)].

B. Breakdown time scale

Analyzing the time-dependent ratio $D(\Delta t)\tau(\Delta t)/T$ (for either rotational or translational motion) allows one to verify quantitatively the role of the time scale in the SE and SED ratios. To contrast the behavior of $D(\Delta t)\tau(\Delta t)/T$ with the average over the entire system, we define the time-dependent "breakdown" ratios as follows:

$$b_{TH}(\Delta t) \equiv \frac{[D(\Delta t)\tau(\Delta t)/T]_{TH}}{[D(\Delta t)\tau(\Delta t)/T]_{all}} \tag{16}$$

and similarly

$$b_{RH}(\Delta t) \equiv \frac{[D(\Delta t)\tau(\Delta t)/T]_{RH}}{[D(\Delta t)\tau(\Delta t)/T]_{all}}. \tag{17}$$

If the DH are related to the breakdown of the SE and SED relations, then one would expect the following (i) The b_{TH} and b_{RH} ratios will show the largest deviations from the system average behavior at the time scale when DH are most pronounced, i.e., approximately at a time that we denote as t^*, at which the non-Gaussian parameter is a maximum (see Appendix C). (ii) The lower T, the larger is the peak of b_{DH} (in agreement with the fact that the DH are more pronounced as T decreases). Figure 5(a) for TH and Fig. 5(b) for RH show the behavior of $b_{DH}(\Delta t)$ for the fastest subset of molecules, for different temperatures. Both expectations (i) and (ii) agree with Fig. 5.

From Fig. 5 we can extract the time t_b when $b_{DH}(\Delta t)$ is a maximum. Figure 6(a) shows t_b for each of the four subsets: TH fastest and slowest and RH fastest and slowest. If DH play a significant role in the breakdown of the SE and SED relations, we would expect that the maximum contribution to
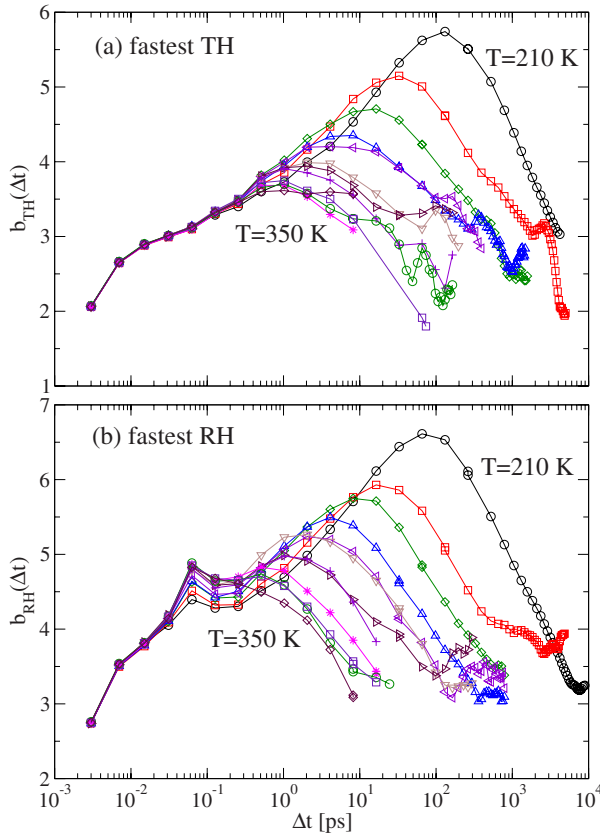
FIG. 5. (Color online) (a) Time-dependent extension $b_{TH}(\Delta t)$ of the Stokes-Einstein relation for the fastest translational heterogeneities (TH) at different T. For the sake of clarity the curve corresponding to $T=290$ K was removed. (b) Time-dependent extension $b_{RH}(\Delta t)$ of the Stokes-Einstein-Debye relation for the fastest rotational heterogeneities (RH) at different T. For the sake of clarity the curve corresponding to $T=290$ K was removed. In both (a) and (b), the maxima occur at the time scales corresponding to the end of the cage regime, when DH are more pronounced. These maxima increase upon cooling, as the DH become more pronounced.

the deviation from the SE and SED relations, occurring at t_b, coincides roughly with the "classical" measure of the characteristic time of DH, t^*. Comparison of Figs. 6(a) and 6(b) for $T<280$ K shows that t^* is slightly larger than t_b for the slowest DH, while is shorter than t_b for fastest DH. Nonetheless, t_b and t^* are approximately the same, and so the largest contribution to the SE and SED ratios is on the time scale when DH are most pronounced. This provides direct evidence for the idea that the appearance of DH is accompanied by the failure of the SE and SED ratios.

C. Decoupling time scales

We next directly probe the relation between DH and the decoupling of D_r and D_t. As discussed above, the time scale at which the DH are observable is much smaller than the time scale at which the system is considered diffusive. Therefore, in analogy to the previous section, we incorporate a time scale in the D_r/D_t ratio so that we can compare the decoupling between rotation and translation at the time scale of the DH. To this end we introduce the ratios
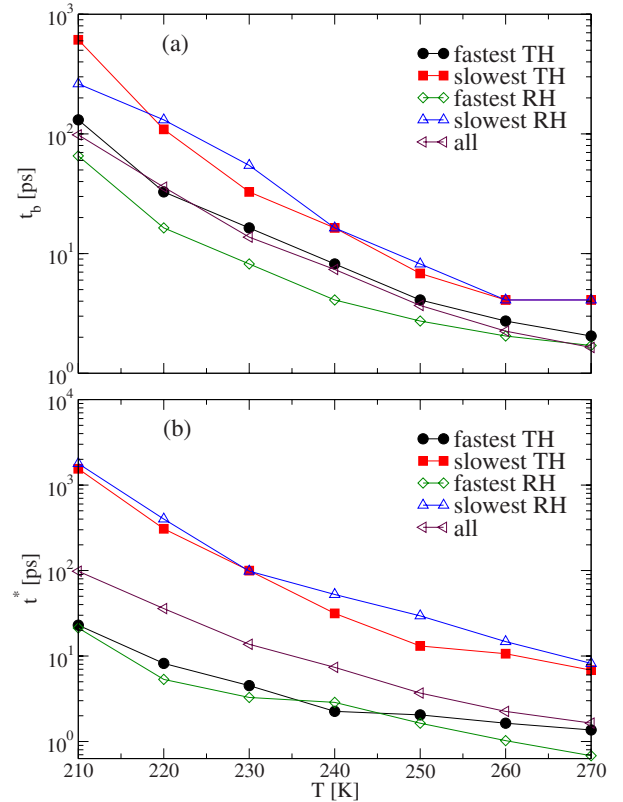

FIG. 6. (Color online) Temperature dependence of (a) t_b, the time at which the time-dependent extensions of the Stokes-Einstein and Stokes-Einstein-Debye relations, b_{TH} and b_{RH}, respectively, have maxima, and (b) t^*, the time at which the non-Gaussian parameter $\alpha_2(\Delta t)$ reaches a maximum. t^* indicates the time scale corresponding to the end of the cage regime. We show the results when considering molecules belonging to translational heterogeneities, rotational heterogeneities, and also for the entire system.

$$d_{TH}(\Delta t) \equiv \frac{[D_r(\Delta t)/D_t(\Delta t)]_{TH}}{[D_r(\Delta t)/D_t(\Delta t)]_{all}}, \qquad (18)$$

and similarly

$$d_{RH}(\Delta t) \equiv \frac{[D_r(\Delta t)/D_t(\Delta t)]_{RH}}{[D_r(\Delta t)/D_t(\Delta t)]_{all}}. \qquad (19)$$

Figure 7(a) shows the results for $d_{TH}(\Delta t)$ for the fastest subsets of molecules. For short times, $d_{TH}(\Delta t)$ does not depend on time and temperature, since in this initial temporal regime the dynamics at all temperatures is ballistic, i.e., both $\langle \varphi^2(\Delta t) \rangle$ and $\langle r^2(\Delta t) \rangle$ are approximately linear with $(\Delta t)^2$. At intermediate times $d_{TH}(\Delta t)$ develops a distinct maximum which increases in magnitude and shifts to larger observation times as T is reduced. The maximum occurs at the time scale where the fastest molecules of the TH and RH "break their cages" and enter the corresponding diffusive regimes [see Fig. 6(b)]. Therefore, the results of Fig. 7(a) also suggest that the decoupling between rotational and translational motion is largest at approximately the same time scale at which the DH are most pronounced. We note from Fig. 7(a) that $d_{TH}(\Delta t) < 1$, indicating that the decoupling of rotational and transla-
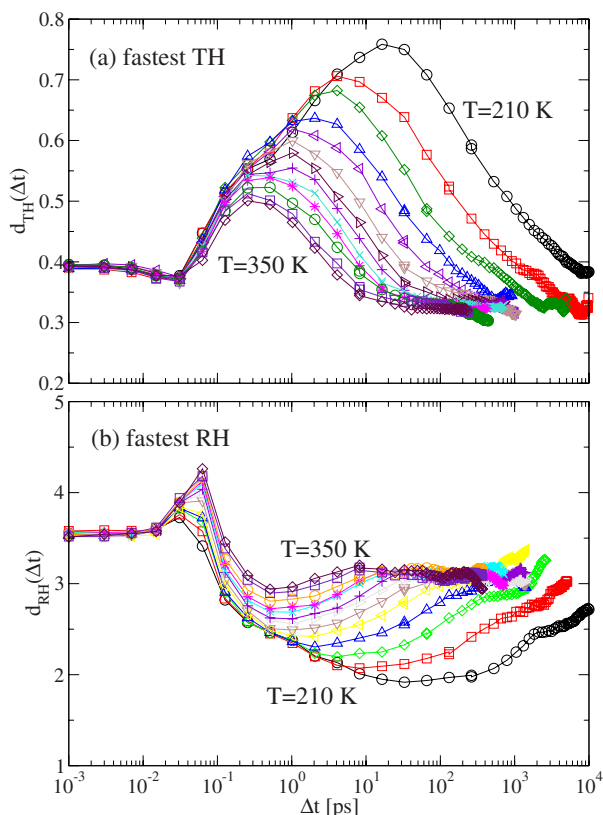
FIG. 7. (Color online) (a) Temporal behavior of the ratio of the time-dependent rotational diffusivity and translational diffusivity for the fastest translational heterogeneities (TH), normalized by the average over the entire system. We show all the simulated temperatures. (b) Temporal behavior of the ratio of the time-dependent rotational diffusivity and translational diffusivity for the fastest rotational heterogeneities (RH), normalized by the average over the entire system. We show all the simulated temperatures. The figure shows that the decoupling of rotation from translation is increasingly more pronounced as T decreases and is a maximum (a) or minimum (b) on the time scale of the DH.

tional motion observed in the fastest subsets of TH is smaller than that from the average over the entire system. As we focus in slower subsets of TH for the same T, we observe that the maximum in $d_{TH}(\Delta t)$ decreases at any given T.

Figure 7(b) shows $d_{RH}(\Delta t)$ for the fastest subsets of molecules. Similarly to the behavior of $d_{TH}(\Delta t)$, at short times $d_{RH}(\Delta t)$ does not depend on time or temperature; molecules move ballistically in this regime. The maxima in $d_{RH}(\Delta t)$ at $\Delta t \approx 0.1$ ps for all temperatures are a consequence of the librational molecular motion, enhanced in this case because we are selecting the fastest subset of RH. At intermediate times, we observe a broad minimum in $d_{RH}(\Delta t)$ centered at $\Delta t \approx t^*$; this minimum becomes deeper and shifts to later times upon cooling, suggesting that the decoupling in the fastest subset of RH is largest at approximately the same time scale at which the DH are more pronounced. The fact that $d_{TH}(\Delta t)$ shows a maximum at approximately t^*, while $d_{RH}(\Delta t)$ shows a minimum at t^* is because the fastest subsets of RH tend to enhance the rotational motion with respect to the translational motion, while the opposite situation occurs

for the fastest subsets of TH. We note from Fig. 7(b) that $d_{RH}(\Delta t) > 1$, indicating that the decoupling of rotational and translational motion observed in the fastest subsets of RH is larger than that found in the average over the entire system.

In short, the behavior of $d_{TH}(\Delta t)$ and $d_{RH}(\Delta t)$ indicates that the emergence of DH is correlated to the rotation and translation decoupling, just as it does for the breakdown of the SE and SED relations.

VII. SUMMARY

In this work, we tested in the SPC/E model for water (i) the validity of the SE and SED equations, (ii) the decoupling of rotational and translational motion, and (iii) the relation of (i) and (ii) to DH. We found that at low temperatures there is a breakdown of both the SE and SED relations and that these relations can be replaced by fractional functional forms. The SE breakdown is observed in every scale of translational mobility. Similarly, the SED breakdown is observed in every scale of rotational mobility. Many believe that the origin of the breakdown of the SE and SED relations can be attributed to the most mobile molecules embedded in an inactive background where these relations hold. Instead our results support the view of a generalized breakdown.

We also found that, upon cooling, there is a decoupling of translational and rotational motion. This decoupling is also observed in all scales of rotational and translational mobilities. In agreement with MD simulations of an OTP model [92], we find that an opposite decoupling is observed depending on whether one uses the rotational diffusivity D_r or the rotational relaxation time τ_2. In the first case, rotational motion is enhanced upon cooling with respect to the translational motion, while the opposite situation holds when choosing τ_2. This is particularly relevant for experiments, where typically only τ_2 is accessible.

We also found that as the decoupling of D_r/D_t increases, the number of molecules belonging simultaneously to both RH and TH also increases. This is counterintuitive since a stronger decoupling would suggest less overlapping of TH and RH. Therefore we conclude that the decoupling of D_r/D_t is significant even at the single-molecule level.

We also explored the role of time scales in the breakdown of the SE and SED relations and decoupling. To do this we introduced time-dependent versions of the SE and SED expressions. Our results suggest that both the decoupling and SE and SED breakdowns are originated at a time scale corresponding to the end of the cage regime, when diffusion starts. This is also the time scale at which the DH are more relevant.

Our work also demonstrates that selecting DH on the basis of translational or rotational displacement more strongly biases the calculation of diffusion constants than the other dynamical properties. If appropriate care is taken, this should not be problematic, but it does make apparent that an alternative approach to identify DH would be valuable. This is especially true when contrasting the behavior of diffusion constants and relaxation times, as is the case for the SE and SED relations.
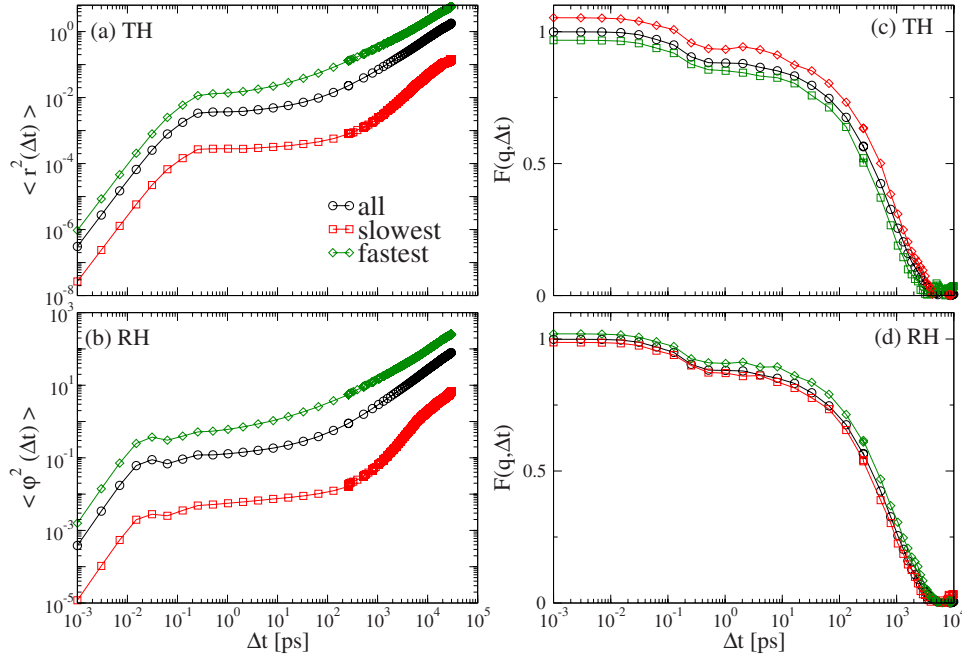
FIG. 8. (Color online) Example of time correlation functions limited to subsets of DH. (a) Mean square displacement (MSD) and (b) rotational mean square displacement (RMSD) at $T=210$ K for the fastest and slowest translational heterogeneities (TH) and rotational heterogeneities (RH), respectively, as well as for the entire system. Intermediate scattering function $F(q, \Delta t)$ at $T=210$ K for (c) the fastest and slowest TH, and entire system and (d) the fastest and slowest RH and the entire system.

APPENDIX A: EVALUATION OF THE ROTATIONAL MEAN SQUARE DISPLACEMENT

To calculate D_r [Eq. (7)] we consider the behavior of the normalized polarization vector $\hat{p}_i(t)$ for molecule i (defined as the normalized vector from the center of mass of the water molecule to the midpoint of the line joining the two hydrogens). The molecular rotation will cause a rotation of $\hat{p}_i(t)$. A naive definition of angular displacement as $\hat{p}_i(t) - \hat{p}_i(0)$ would be insensitive to full molecular rotations, since it would result in a bounded quantity. Following Ref. [71], we avoid this complication by defining the vector rotational displacement in the time interval $[t, t+\Delta t]$ as

$$\vec{\varphi}_i(\Delta t) \equiv \int_t^{t+\Delta t} \Delta \vec{\varphi}_i(t') dt', \tag{A1}$$

where $\Delta \vec{\varphi}_i(t')$ is a vector with direction given by $\hat{p}_i(t') \times \hat{p}_i(t'+dt')$ and with magnitude given by $|\Delta \vec{\varphi}_i(t')| \equiv \cos^{-1}(\hat{p}_i(t') \cdot \hat{p}_i(t'+dt'))$, i.e., the angle spanned by $\hat{p}_i$ in the time interval $[t', t'+dt']$. Thus, the vector $\vec{\varphi}_i(\Delta t)$ allows us to define a trajectory in a three-dimensional space representing the rotational motion of molecule i, analogous to the trajectory defined by $\vec{r}_i(\Delta t)$ for the translational case. We define, in analogy to the MSD, a *rotational* mean square displacement (RMSD) [18,71,74]

$$\langle \varphi^2(\Delta t) \rangle \equiv \frac{1}{N} \sum_{i=0}^{N} |\vec{\varphi}_i(t + \Delta t) - \vec{\varphi}_i(t)|^2. \tag{A2}$$

Using this form, we define D_r as given by Eq. (7), analogous to the definition of D_t. We have verified that there is no qualitative difference in the results of the present work, when the polarization vector is replaced by the other two principal directions of the water molecule.

APPENDIX B: CORRELATION FUNCTIONS FOR DYNAMICAL HETEROGENEITIES

We introduce a MSD $\langle r^2(\Delta t) \rangle$ for the fastest and slowest subsets of molecules by limiting the sum in Eq. (6) to the molecules in the corresponding subset at time Δt. The different MSDs at $T=210$ K are shown in Fig. 8(a). We note that, since the most and least mobile 7% of the molecules will generally vary as a function of time, the molecules used to calculate $\langle r^2(\Delta t) \rangle$ will change with time; in other words, when a molecule ceases being part of a DH, it is no longer considered in the computation of the MSD and the focus is shifted to the new subset of molecules belonging to the DH considered. Analyzing the $\langle r^2(\Delta t) \rangle$ for the collection of subsets from most mobile to least mobile has the advantage that the mean of $\langle r^2(\Delta t) \rangle$ over the subsets converges to the MSD for the full system. In a similar fashion the RMSD $\langle \varphi^2(\Delta t) \rangle$ is calculated also for the fastest and slowest rotationally mobile molecules [Fig. 8(b)].

To complement the single-particle dynamics determined by $\langle r^2(\Delta t) \rangle$ and $\langle \varphi^2(\Delta t) \rangle$, we also evaluate the coherent intermediate scattering function

$$F(q, \Delta t) \equiv \frac{1}{NS(q)} \sum_{j=1}^{N} e^{-iqr_j(t+\Delta t)} \sum_{k=1}^{N} e^{iqr_k(t)}, \quad \text{(B1)}$$

where $S(q)$ is the structure factor. $F(q, \Delta t)$ reflects two-particle temporal correlations instead of single-particle correlations (as in the case of the MSD). The normalization factors ensure that $F(q, 0) = 1$. In analogy to our analysis of $\langle r^2(\Delta t) \rangle$, we would like to evaluate the contribution to $F(q, \Delta t)$ made by subsets of molecules. Naively, one might think this can be simply done by limiting the sums in Eq. (B1) to solely those molecules within the subset. However, taking the mean over the subsets of such a quantity will not recover the complete $F(q, \Delta t)$, since there will be no information on the cross correlations between the subsets. In order to include these correlations and define a function that, when averaged over subsets, will return $F(q, \Delta t)$ (as is the case for the MSD and RMSD), we simply limit one of the two sums to the subset, while the other sum still extends over all molecules. Mathematically, we define

$$F_{\text{subset}}(q, \Delta t) \equiv \frac{1}{N_{\text{subset}}S(q)} \sum_{j=1}^{N} e^{-iqr_j(t+\Delta t)} \sum_{k \in subset} e^{iqr_k(t)}. \quad \text{(B2)}$$

Note that one must make the choice whether to limit the sum to the subset at time t or $t + \Delta t$; we have found that in practice there is little, if any, qualitative difference in this choice. Thus we measure the correlations between the subset of molecules at time t with all molecules at time $t + \Delta t$. Additionally, $F_{\text{subset}}(q, 0)$ is not necessarily 1; forcing this normalization would not satisfy the desired condition that the mean over subsets returns the average over all molecules. In all cases, we evaluate $F_{\text{subset}}(q, \Delta t)$ at $q = 18$ nm^{-1}, the value of the transferred momentum at the first maximum of the structure factor where the relaxation is slowest (except for the $q \to 0$ limit). Figures 8(c) and 8(d) show $F(q, \Delta t)$ for all molecules, and for the fastest and the slowest TH and RH.

At this point, it is important to compare the behavior of $\langle r^2(\Delta t) \rangle$ and $\langle \varphi^2(\Delta t) \rangle$ with that of $F(q, \Delta t)$ for the TH and RH subsets. Since we define mobility on the basis of displacement, the behavior of $\langle r^2(\Delta t) \rangle$ and $\langle \varphi^2(\Delta t) \rangle$ for the subsets are much more strongly affected than $F_{\text{subset}}(q, \Delta t)$ for the subsets. Additionally, $F_{\text{subset}}(q, \Delta t)$ includes cross correlations both within and between subsets that a single-particle definition of mobility does not include. More specifically, the results in Fig. 8 at $T = 210$ K show that there is roughly two orders of magnitude difference between $\langle r^2(\Delta t) \rangle$ for the most and least mobile molecules [and similar difference for $\langle \varphi^2(\Delta t) \rangle$]. We also find that there is roughly also two orders of magnitude difference between the most and least mobile molecules for D_t and D_r. For higher T, the difference is less pronounced. When we examine the relaxation of $F(q, \Delta t)$ for the most and least mobile subsets, we find only a difference of a factor of ≈ 2 between the time scales for relaxation. Therefore—not surprisingly—selecting mobility based on single-particle displacement results in a much stronger effect
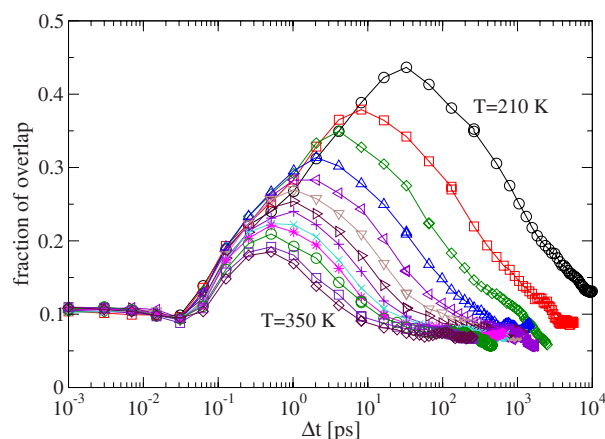

FIG. 9. (Color online) Fraction of molecules belonging simultaneously to both fastest translational heterogeneities (TH) and fastest rotational heterogeneities (RH) versus observation time Δt, at different temperatures. This overlap of fastest TH and fastest RH is maximum at the end of the cage regime and increases upon cooling. It is almost 45% at the lowest T.

on diffusion than it does for collective relaxation phenomena. This fact is important for the comparison between this work and a previous work [22].

APPENDIX C: CHARACTERISTIC TIME OF DYNAMICAL HETEROGENEITIES

Since we analyze the DH in the context of both translational and rotational motions, it is natural to ask at what time scale the TH and RH are more pronounced and to what degree the TH and RH subsets overlap each other. References [63,74] show that the fastest subsets of TH and RH form clusters, and that these clusters are larger at approximately the time t^* corresponding to the onset of the diffusive regime, as indicated by $\langle r^2(\Delta t) \rangle$ and $\langle \varphi^2(\Delta t) \rangle$, respectively. Normally t^* for the translational case is defined as the maximum in the non-Gaussian parameter [94]

$$\alpha_2(\Delta t) \equiv \frac{3 \langle r^4(\Delta t) \rangle}{5 \langle r^2(\Delta t) \rangle} - 1, \quad \text{(C1)}$$

where $\langle r^4(\Delta t) \rangle$ and $\langle r^2(\Delta t) \rangle$ are the fourth and second moments of the displacement distribution, respectively (the latter is also the MSD). $\alpha_2(\Delta t)$ is known to be identically zero for a Gaussian distribution, and thus it signals when the dynamics does not generate such a Gaussian distribution of displacements. In the present study, we use either translational, $\vec{r}_i(\Delta t)$, or rotational, $\vec{\varphi}_i(\Delta t)$, displacement for TH and RH, respectively, when computing $\alpha_2(\Delta t)$. Figure 6(b) shows t^* as a function of T defined for the fastest and slowest subsets of both the TH and RH. We also include the corresponding values of t^* for the entire system. Figure 6(b) shows that there is no qualitative difference in shape of the curve of $t^*(T)$ for the different subsets considered and the entire system.

Since the values of t^* for TH and RH are similar, we expect that there is some coupling between TH and RH.

Previously, Chen *et al.* [95] found that at large momentum transfer q, there is coupling between translational and rotational motion. The maximum correlation occurs at the cage relaxation time t^* for large values of q. Reference [74] found a spatial correlation between RH and TH. Along similar lines, we examine the overlap between these subsets. Figure 9 shows the overlap between the fastest subset of molecules belonging to TH and RH, as a function of Δt and T. Specifically, we count the number of fastest molecules belonging simultaneously to TH and RH as a function of observation time Δt. Similar to Fig. 9 in Ref. [95], the strength of this coupling reaches its maximum at the cage relaxation times, but these times are consistently shorter than those reported in [95]; this is likely to be due to the fact that we consider fastest TH and fastest RH in this calculation, while Ref. [95] considers all the molecules of the system. Figure 9 indicates that, at the lowest temperature simulated, about 45% of the molecules comprising the fastest subset of TH coincide with the ones in the fastest subset of RH.

[1] A. Einstein, *Investigations on the Theory of the Brownian Motion* (Dover, New York, 1956).

[2] P. Debye, *Polar Molecules* (Dover, New York, 1929).

[3] R. A. L. Jones, *Soft Condensed Matter* (Oxford University Press, Oxford, 2002).

[4] L. Andreozzi, M. Bagnoli, M. Faetti, and M. Giordano, J. Non-Cryst. Solids **303**, 262 (2002).

[5] E. Rössler, Phys. Rev. Lett. **65**, 1595 (1990).

[6] S. F. Swallen, P. A. Bonvallet, R. J. McMahon and M. D. Ediger, Phys. Rev. Lett. **90**, 015901 (2003).

[7] M. T. Cicerone, F. R. Blackburn and M. D. Ediger, J. Chem. Phys. **102**, 471 (1995); F. R. Blackburn, C.-Y. Wang, and M. D. Ediger, J. Phys. Chem. **100**, 18249 (1996).

[8] S.-H. Chen, F. Mallamace, C.-Y. Mou, M. Broccio, C. Corsaro, A. Faraone, and L. Liu, Proc. Natl. Acad. Sci. U.S.A. **103**, 12974 (2006).

[9] B. Chen, E. E. Sigmund, and W. P. Halperin, Phys. Rev. Lett. **96**, 145502 (2006).

[10] F. H. Stillinger and J. A. Hodgdon, Phys. Rev. E **50**, 2064 (1994).

[11] J. F. Douglas and D. Leporini, J. Non-Cryst. Solids **235–237**, 137 (1998).

[12] K. L. Ngai, J. Phys. Chem. B **103**, 10684 (1999).

[13] J. Kim and T. Keyes, J. Phys. Chem. B **109**, 21445 (2005).

[14] T. Franosch, M. Fuchs, W. Götze, M. R. Mayr, and A. P. Singh, Phys. Rev. E **56**, 5659 (1997).

[15] G. Tarjus and D. Kivelson, J. Chem. Phys. **103**, 3071 (1995).

[16] M. Nicodemi and A. Coniglio, Phys. Rev. E **57**, R39 (1998).

[17] K. S. Schweizer and E. J. Saltzman, J. Phys. Chem. B **108**, 19729 (2004).

[18] C. De Michele and D. Leporini, Phys. Rev. E **63**, 036702 (2001).

[19] P. A. Netz, F. W. Starr, H. E. Stanley, and M. C. Barbosa, J. Chem. Phys. **115**, 344 (2001); P. A. Netz, M. C. Barbosa and H. E. Stanley, J. Mol. Liq. **101**, 159 (2002); P. A. Netz, S. V. Buldyrev, M. C. Barbosa, and H. E. Stanley, Phys. Rev. E **73**, 061504 (2006); P. A. Netz, F. W. Starr, M. C. Barbosa, and H. E. Stanley, Physica A **314**, 470 (2002).

[20] G. Matsui and S. Kojima, Phys. Lett. A **293**, 156 (2002).

[21] J. Qian, R. Hentschke, and A. Heuer, J. Chem. Phys. **110**, 4514 (1999).

[22] S. R. Becker, P. H. Poole, and F. W. Starr, Phys. Rev. Lett. **97**, 055901 (2006).

[23] L. Berthier, D. Chandler, and J. P. Garrahan, Europhys. Lett. **69**, 320 (2005).

[24] S. K. Kumar, G. Szamel, and J. F. Douglas, J. Chem. Phys. **124**, 214501 (2006).

[25] M. Dzugutov, S. I. Simdyankin, and F. H. M. Zetterling, Phys. Rev. Lett. **89**, 195701 (2002).

[26] P. Bordat, F. Affouard, M. Descamps, and F. Müller-Plathe, J. Phys.: Condens. Matter **15**, 5397 (2003).

[27] P. Kumar, Proc. Natl. Acad. Sci. U.S.A. **103**, 12955 (2006).

[28] P. Kumar, S. V. Buldyrev, S. R. Becker, F. W. Starr, P. H. Poole, and H. E. Stanley, Proc. Natl. Acad. Sci. U.S.A. **104**, 9575 (2007).

[29] Y.-J. Jung, J. P. Garrahan, and D. Chandler, Phys. Rev. E **69**, 061205 (2004).

[30] L. Xu, F. Mallamace, Z. Yan, F. W. Starr, S. V. Buldyrev, and H. E. Stanley, preprint (2007).

[31] M. D. Ediger, Annu. Rev. Phys. Chem. **51**, 99 (2000).

[32] H. Sillescu, J. Non-Cryst. Solids **243**, 81 (1999).

[33] I. Chang and H. Sillescu, J. Phys. Chem. B **101**, 8794 (1997).

[34] A. Döß, G. Hinze, B. Schiener, J. Hemberger, and R. Böhmer, J. Chem. Phys. **107**, 1740 (1997).

[35] W. Steffen, A. Patkowski, G. Meier, and E. W. Fischer, J. Chem. Phys. **96**, 4171 (1992).

[36] E. W. Fischer, E. Donth, and W. Steffen, Phys. Rev. Lett. **68**, 2344 (1992).

[37] C. A. Angell, Science **267**, 1924 (1995).

[38] T. Loerting and N. Giovambattista, J. Phys.: Condens. Matter **18**, R919 (2006).

[39] M. D. Ediger, C. A. Angell, and S. R. Nagel, J. Phys. Chem. **100**, 13200 (1996).

[40] P. G. Debenedetti, *Metastable Liquids* (Princeton University Press, Princeton, 1996).

[41] E. R. Weeks, J. C. Crocker, A. C. Levitt, A. Schofield, and D. A. Weitz, Science **287**, 627 (2000).

[42] R. Böhmer, R. V. Chamberlin, G. Diezemann, B. Geil, A. Heuer, G. Hinze, S. C. Kuebler, R. Richert, B. Schiener, H. Sillescu, H. W. Spiess, U. Tracht, and M. Wilhelm, J. Non-Cryst. Solids **235–237**, 1 (1998).

[43] U. Tracht, M. Wilhelm, A. Heuer, H. Feng, K. Schmidt-Rohr, and H. W. Spiess, Phys. Rev. Lett. **81**, 2727 (1998).

[44] L. A. Deschenes and D. A. Vanden Bout, Science **292**, 255 (2001).

[45] L. A. Deschenes and D. A. Vanden Bout, J. Phys. Chem. B **106**, 11438 (2002).

[46] A. S. Keys, A. Abate, S. C. Glotzer, and D. J. Durian, Nat. Phys. **3**, 260 (2007).

[47] R. Richert, J. Phys.: Condens. Matter **14**, R703 (2002).

[48] S. C. Glotzer, J. Non-Cryst. Solids **274**, 342 (2000).

[49] S. A. Kivelson, X.-C. Zeng, D. Kivelson, C. M. Knobler, and T. Fischer, J. Chem. Phys. **101**, 2391 (1994).

[50] K. Y. Tsang and K. L. Ngai, Phys. Rev. E **54**, R3067 (1996).

[51] C. Bennemann, C. Donati, J. Baschnagel, and S. C. Glotzer, Nature (London) **399**, 246 (1999).

[52] Y. Gebremichael, T. B. Schrøder, F. W. Starr, and S. C. Glotzer, Phys. Rev. E **64**, 051503 (2001).

[53] C. Donati, S. C. Glotzer, and P. H. Poole, Phys. Rev. Lett. **82**, 5064 (1999); N. Lačević, F. W. Starr, T. B. Schrøder, V. N. Novikov, and S. C. Glotzer, Phys. Rev. E **66**, 030101(R) (2002); N. Lačević, F. W. Starr, T. B. Schrøder, and S. C. Glotzer, J. Chem. Phys. **119**, 7372 (2003).

[54] Y. Gebremichael, M. Vogel, M. N. J. Bergroth, F. W. Starr, and S. C. Glotzer, J. Phys. Chem. B **109**, 15068 (2005).

[55] M. Vogel and S. C. Glotzer, Phys. Rev. Lett. **92**, 255901 (2004); Phys. Rev. E **70**, 061504 (2004).

[56] Y. Gebremichael, M. Vogel, and S. C. Glotzer, J. Chem. Phys. **120**, 4415 (2004).

[57] First suggested by G. Tammann, *Der Glasszustand* (Leopold Voss, Leipzig, 1933).

[58] M. M. Hurley and P. Harrowell, Phys. Rev. E **52**, 1694 (1995); D. N. Perera and P. Harrowell, J. Chem. Phys. **111**, 5441 (1999); Phys. Rev. Lett. **81**, 120 (1998); A. Widmer-Cooper, P. Harrowell, and H. Fynewever, *ibid.* **93**, 135701 (2004); A. Widmer-Cooper and P. Harrowell, *ibid.* **96**, 185701 (2006).

[59] A. I. Mel'cuk, R. A. Ramos, H. Gould, W. Klein, and R. D. Mountain, Phys. Rev. Lett. **75**, 2522 (1995).

[60] A. C. Pan, J. P. Garrahan, and D. Chandler, Phys. Rev. E **72**, 041106 (2005).

[61] M. S. Shell, P. G. Debenedetti, and F. H. Stillinger, J. Phys.: Condens. Matter **17**, S4035 (2005).

[62] W. Kob, C. Donati, S. J. Plimpton, P. H. Poole, and S. C. Glotzer, Phys. Rev. Lett. **79**, 2827 (1997); C. Donati, J. F. Douglas, W. Kob, S. J. Plimpton, P. H. Poole, and S. C. Glotzer, *ibid.* **80**, 2338 (1998).

[63] N. Giovambattista, S. V. Buldyrev, F. W. Starr, and H. E. Stanley, Phys. Rev. Lett. **90**, 085506 (2003).

[64] S. C. Glotzer, V. Novikov, and T. B. Schrøder, J. Chem. Phys. **112**, 509 (2000).

[65] K. Vollmayr-Lee, W. Kob, K. Binder, and A. Zippelius, J. Chem. Phys. **116**, 5158 (2002).

[66] G. S. Matharoo, M. S. Gulam Razul, and P. H. Poole, Phys. Rev. E **74**, 050502(R) (2006).

[67] G. Adam and J. H. Gibbs, J. Chem. Phys. **43**, 139 (1965).

[68] J. D. Stevenson, J. Schmalian, and P. G. Wolynes, Nat. Phys. **2**, 268 (2006).

[69] J. R. Errington, P. G. Debenedetti, and S. Torquato, Phys. Rev. Lett. **89**, 215503 (2002).

[70] A. Geiger and H. E. Stanley, Phys. Rev. Lett. **49**, 1749 (1982).

[71] S. Kammerer, W. Kob, and R. Schilling, Phys. Rev. E **56**, 5450 (1997).

[72] J. Kim and T. Keyes, J. Chem. Phys. **121**, 4237 (2004).

[73] J. Kim, W.-X. Li, and T. Keyes, Phys. Rev. E **67**, 021506 (2003).

[74] M. G. Mazza, N. Giovambattista, F. W. Starr, and H. E. Stanley, Phys. Rev. Lett. **96**, 057803 (2006).

[75] H. J. C. Berendsen, J. R. Grigera, and T. P. Stroatsma, J. Phys. Chem. **91**, 6269 (1987).

[76] O. Steinhauser, Mol. Phys. **45**, 335 (1982).

[77] H. J. C. Berendsen, J. P. M. Postma, W. F. van Gunsteren, A. DiNola, and J. R. Haak, J. Chem. Phys. **81**, 3684 (1984).

[78] Although it is desirable to simulate in the microcanonical ensemble (*NVE*), for long simulations a small energy drift is unavoidable. To correct this situation, the Berendsen thermostat was employed with a very long time constant $\tau = 200$ ps. For an interesting discussion on the relation between the Berendsen thermostat and canonical and microcanonical ensembles, see T. Morishita, J. Chem. Phys. **113**, 2976 (2000).

[79] F. W. Starr, F. Sciortino, and H. E. Stanley, Phys. Rev. E **60**, 6757 (1999).

[80] J. P. Hansen and I. R. McDonald, *Theory of Simple Liquids* (Academic Press, London, 2006).

[81] E. W. Lang, D. Girlich, H.-D. Lüdemann, L. Piculell, and D. Müller, J. Chem. Phys. **93**, 4796 (1990).

[82] F. Fernandez-Alonso, F. J. Bermejo, S. E. McLain, J. F. C. Turner, J. J. Molaison, and K. W. Herwig, Phys. Rev. Lett. **98**, 077801 (2007).

[83] C. Donati, S. C. Glotzer, P. H. Poole, W. Kob, and S. J. Plimpton, Phys. Rev. E **60**, 3107 (1999).

[84] G. L. Pollack, Phys. Rev. A **23**, 2660 (1981); G. L. Pollack, and J. J. Enyeart, *ibid.* **31**, 980 (1985).

[85] M. T. Cicerone and M. D. Ediger, J. Chem. Phys. **104**, 7210 (1996).

[86] L. Bocquet, J. P. Hensen, and J. Piasecki, J. Stat. Phys. **76**, 527 (1994).

[87] A. Voronel, E. Veliyulin, V. Sh. Machavariani, A. Kisliuk, and D. Quitmann, Phys. Rev. Lett. **80**, 2630 (1998).

[88] L. Andreozzi, A. Di Schino, M. Giordano, and D. Leporini, Europhys. Lett. **38**, 669 (1997).

[89] S. H. Bielowka, T. Psurek, J. Ziolo, and M. Paluch, Phys. Rev. E **63**, 062301 (2001); T. Psurek, S. Hensel-Bielowka, J. Ziolo, and M. Paluch, J. Chem. Phys. **116**, 9882 (2002).

[90] F. H. Stillinger and A. Rahman, J. Chem. Phys. **60**, 1545 (1974).

[91] L. Berthier, Phys. Rev. E **69**, 020201(R) (2004).

[92] T. G. Lombardo, P. G. Debenedetti, and F. H. Stillinger, J. Chem. Phys. **125**, 174507 (2006).

[93] Assuming a Kohlrausch form for the intermediate scattering function, $\exp(-t/\tau)^\beta$, the integral will yield $\tau(\infty) = \tau\Gamma(\beta^{-1})/\beta$, where $\Gamma(x)$ is the Euler Gamma function.

[94] A. Rahman, Phys. Rev. **136**, A405 (1964).

[95] For a discussion on the same question from the point of view of the intermediate scattering function, see S.-H. Chen, P. Gallo, F. Sciortino, and P. Tartaglia, Phys. Rev. E **56**, 4231 (1997).